Concept of Dual-Band and Multistage Bandpass Filters with Antiparallel Configuration

Siniša Jovanović, Bratislav Milovanović[1]

Abstract – **This paper explores the application of band pass filters with antiparallel configurations for obtaining dual band filters of compact sizes and various characteristics. It also outlines the theoretical analysis of higher-order filters obtained by the cascading of the identical basic filters. The previously developed model for filters with antiparallel configuration is enhanced by replacing the ideal inductances with transmission lines. The characteristic impedance of the transmission lines is introduced as an additional independent parameter that affects the occurrences and the position of the parasitic passband at higher frequencies. This property is implemented within a program for electrical circuit simulation to obtain a model of dual band bandpass filter with tuneable characteristics and a simultaneous calculation of values for all components of an ideal circuit model. The analysis of higher-order filters demonstrated that two possible multistage topologies have identical electrical characteristics but different practical applicability. An iterative formula for frequency characteristics calculation as well as formulas for the frequency position of transmission zeros and poles are developed. The component values of the filter prototypes calculated by these theoretical studies can be scaled to obtain band pass filters with various usable characteristics at arbitrary microwave frequencies suitable for realization in various technologies.**

Keywords – **Band Pass Filter, Antiparallel Configuration, Dual Band Filters, Multistage Filters, Microwave Filters.**

I. Introduction

The interest for the design of band pass filters with multiple pass band increased in recent years due to the appearance of advanced multiple-band wireless systems. At the beginning, dual band wireless systems operated at 900 MHz and 1.9 GHz, but later at frequencies of 2.4 GHz and 5.2 GHz. The initial version of the dual band filter was proposed in [1] and contained a parallel combination of two individual bandpass filters with a single passband. Such a solution required the matching circuits for the filter branches and suffered from a large overall size and high insertion loss. In the following years, several designs of dual band filters using various types of resonators were proposed, such as: parallel-coupled resonators [2], ring resonators [3], open-loop resonators [4], stepped-impedance resonators [5] and quarter wavelength resonators [6]. The major challenge in all these cases was to use the same resonator for obtaining the small insertion loss in both passbands as well as a sharp selectivity and good suppression at higher frequencies. Besides the electrical characteristics, equally important requirements were obtaining a small overall filter size and simple construction.

This paper demonstrates that filters with antiparallel configurations, described in [7-10], that were initially used as a standard bandpass, could be used for achieving dual-band characteristics by tuning the values of four independent variables that control the electrical characteristics, without increasing complexity of the basic filter configuration. Better selectivity of both single band and dual band antiparallel filters can be achieved by a simple cascading of identical basic filters with antiparallel configuration.

II. Ideal Filter with Antiparallel Configuration

Filters with antiparallel configurations are introduced in [7]. It was shown that S parameters of an antiparallel connection of two identical asymmetrical subnetworks could be significantly different from the S parameters of a parallel connection of the same subnetworks as well as from the S parameters of the original subnetwork. The antiparallel network could contain additional transmission and reflection zeros and, depending on the subnetwork structure, can have the characteristics of low-pass, high-pass or band-pass filters. The simplest configuration capable of having band-pass frequency characteristics is presented in Fig. 1.

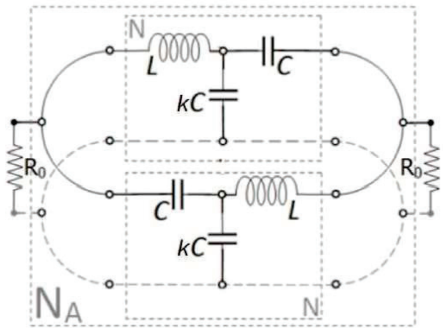

Fig. 1. The simplest configuration of an antiparallel network that could form a bandpass filter [7]

The frequency characteristics of network N_A from Fig.1 are defined by only three parameters: C, L and k. By requesting N_A to be a band pass filter with double S_{11} zeros at ω_c=1, therefore having a normalized central angular frequency, and selecting C as an independent variable, the parameter k can be expressed with a certain approximation discussed in [8] as functions of C:

$$k \approx \sqrt{4C^2 - 1} - 2 - 0.20844 \cdot C^{-3.047732} \quad , \tag{1}$$

Article history: Received September 17, 2018; Accepted November 20, 2018

Siniša Jovanović is with IMTEL Komunikacije, Blvd M. Pupina 165B, 11070 Novi Beograd, Serbia, E-mail: siki@insimtel.com

[1]Bratislav Milovanović is with Singidunum University, Center Niš, Nikole Pašića 28, 18000 Niš, Serbia, E-mail: bmilovanovic@singidunum.ac.rs

while parameter L can be calculated from C and k as:

$$L=\frac{1+k(1+C(C(k+2)+\sqrt{4C^2-(k+2)^2}))}{C(C^2k^2+(k+1)^2)}. \tag{2}$$

In that manner, a prototype family of the basic configuration of an antiparallel band pass filter with the passband centered on the unity angular frequency is defined, having selectivity and passband widths, controlled by independent variable C.

As described in [9], the basic configuration of an antiparallel band pass filter has limited practical applicability. This can be mitigated by extending the filter's configuration with one additional series capacitor and one additional series inductor in series branches of the basic subnetwork as illustrated in Fig. 2.

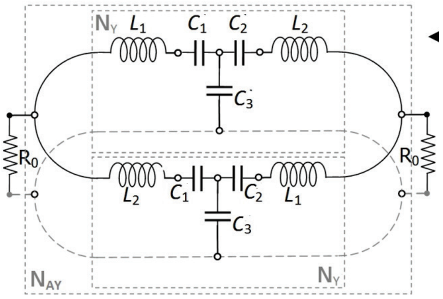

Fig. 2. Configuration of extended antiparallel bandpass filter (EABPF) with Y-connected capacitances [9]

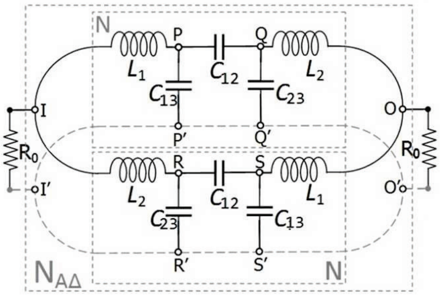

Fig. 3. Configuration of extended antiparallel bandpass filter with Δ-connected capacitances [9]

As shown in [9], the components of N_Y can be defined with the same parameters (C, L, k) used for the basic filter's configuration, with two additional positive parameters (m, n):

$$L_1=(m+1)L, \tag{3}$$

$$L_2=n/C, \tag{4}$$

$$C_1=1/mL, \tag{5}$$

$$C_2=C/(n+1), \tag{6}$$

$$C_3=kC. \tag{7}$$

As shown in [9], parameters m and n are closely related to the angular frequency position of the transmission zero pair (ω_{EZ1}, ω_{EZ2}) which is inherent to extended antiparallel filters.

With certain approximation, parameters m and n can be expressed as a function of ω_{EZ1} and ω_{EZ2}, respectively with the following simple relations:

$$m\approx\frac{[LC(k+1)]^{-1}-\omega_{EZ1}^2}{\omega_{EZ1}^2-1}, \tag{8}$$

$$n\approx\frac{1+k^{-1}}{\omega_{EZ2}^2-1}. \tag{9}$$

The filter configuration from Fig. 2 can be transformed to the configuration shown in Fig. 3 by a Y to Δ transformation of the capacitors. The Δ configuration is more suitable for practical realization as explained in [10]

The values of capacitors of Δ configuration are also defined by the same set of parameters (C, L, k, m, n) with the following expressions:

$$C_{13}=\frac{k(n+1)C}{1+n+m(1+k(n+1))LC} \tag{10}$$

$$C_{23}=\frac{kmC^2L}{1+n+m(1+k(n+1))LC} \tag{11}$$

$$C_{12}=\frac{C}{1+n+m(1+k(n+1))LC} \tag{12}$$

Both Y and Δ filter configurations are mutually electrically compatible. By applying expressions (1), (2), (8) and (9) into expressions (3-7) and (10-12) all components of the filters can be calculated in terms of three independent parameters C, ω_{EZ1} and ω_{EZ2}. The S-parameter frequency responses of the filters can also be expressed in terms of the same three parameters as explained in [9-10]. Fig. 4 shows S-parameter frequency characteristics for several various filters for several values of three independent parameters. It demonstrates that various bandwidths and controlled positions of transmission zeros can be achieved with good accuracy. It also validates the approximate expressions (8) and (9) since the positions of the transmission zeros in Fig. 4 accurately correspond to the given values of ω_{EZ1} and ω_{EZ2}. The increase of C parameter increases the isolation in both the lower and the upper stopband and simultaneously decreases the bandwidth of the passband.

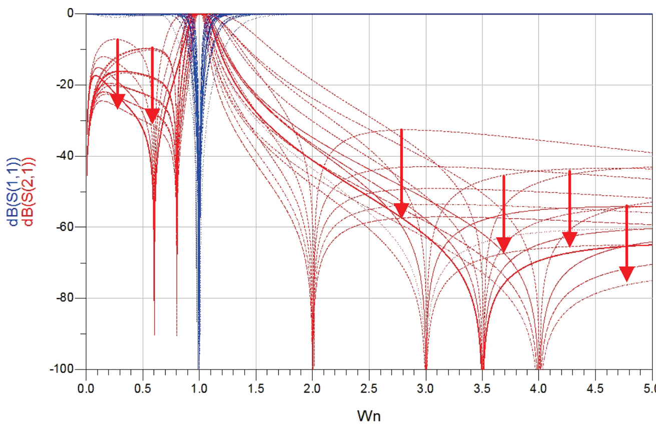

Fig. 4. S-parameter frequency characteristics of the filter model for various combinations of parameter values (C={2, 3, 4, 5}; ω_{EZ1}={0.6, 0.8}; ω_{EZ2}={2, 3, 3.5, 4} [8]. The red arrows indicate the isolation increase with increasing of C

III. Filter with Antiparallel Config. and Transmission Lines as Inductive Elements

Filter realization in some of the planar techniques requires a realization of the filer's components as transmission lines. The corresponding mathematical model of the filter can be obtained by replacing the transmission matrix of the ideal components with a transmission matrix of the corresponding transmission lines. The transmission matrix of the transmission line that substitutes inductances L_1 and L_2 can be expressed with the following equations:

$$\mathbf{T}_{TL_1} = \begin{bmatrix} \cos\frac{(m+1)L\omega}{z_c} & i\cdot z_c \sin\frac{(m+1)L\omega}{z_c} \\ \frac{i}{z_c}\sin\frac{(m+1)L\omega}{z_c} & \cos\frac{(m+1)L\omega}{z_c} \end{bmatrix}, \tag{13}$$

$$\mathbf{T}_{TL_2} = \begin{bmatrix} \cos\frac{n\omega}{z_c C} & i\cdot z_c \sin\frac{n\omega}{z_c C} \\ \frac{i}{z_c}\sin\frac{n\omega}{z_c C} & \cos\frac{n\omega}{z_c C} \end{bmatrix}, \tag{14}$$

where z_c represents the normalized characteristic impedance ($z_c=Z_c/R_0$) of the corresponding transmission line. For practical reasons it is assumed that both transmission lines have the same characteristic impedance. For large values of the relative characteristic impedance z_c the following applies:

$$\lim_{z_c\to\infty} \mathbf{T}_{TL_1} = \begin{bmatrix} 1 & i\omega(m+1)L \\ 0 & 1 \end{bmatrix} = \begin{bmatrix} 1 & i\omega L_1 \\ 0 & 1 \end{bmatrix}, \tag{15}$$

$$\lim_{z_c\to\infty} \mathbf{T}_{TL_2} = \begin{bmatrix} 1 & i\omega\frac{n}{C} \\ 0 & 1 \end{bmatrix} = \begin{bmatrix} 1 & i\omega L_2 \\ 0 & 1 \end{bmatrix}. \tag{16}$$

By employing (13) and (14), the S-parameters matrix of the entire filter can be expressed as:

$$\mathbf{S}_{ETL} = \begin{bmatrix} \frac{SN_{TL1}(C,\omega_{EZ1},\omega_{EZ2},z_c,\omega)}{SD_{TL}(C,\omega_{EZ1},\omega_{EZ2},z_c,\omega)} & i\frac{SN_{TL2}(C,\omega_{EZ1},\omega_{EZ2},z_c,\omega)}{SD_{TL}(C,\omega_{EZ1},\omega_{EZ2},z_c,\omega)} \\ i\frac{SN_{TL2}(C,\omega_{EZ1},\omega_{EZ2},z_c,\omega)}{SD_{TL}(C,\omega_{EZ1},\omega_{EZ2},z_c,\omega)} & \frac{SN_{TL1}(C,\omega_{EZ1},\omega_{EZ2},z_c,\omega)}{SD_{TL}(C,\omega_{EZ1},\omega_{EZ2},z_c,\omega)} \end{bmatrix}, \tag{17}$$

which means that besides C, ω_{EZ1} and ω_{EZ2}, the filter features depend on additional independent parameter z_c. Fig. 5, which is obtained by implementing (17) into [11], shows the dependence of frequency characteristics of the antiparallel filter with inductances replaced with transmission lines due to different values of relative characteristic impedance z_c and for the fixed values of the remaining three independent parameters. The frequency characteristics of the filter with transmission lines having the higher z_c values are very close to the characteristics of a filter composed of ideal components having ω_c=1 and the transmission zeros at exact values set by the input parameters ω_{EZ1} and ω_{EZ2}. The lower values of z_c cause the reduction of the isolation in the upper stopband region and appearance of parasitic passbands at higher frequencies. Lower z_c also causes the shift of the positions of transmission zeros and ω_c toward frequencies lower than ω_{EZ1}, ω_{EZ2} and 1, respectively, due to the influence of the parasitic capacitance of the inductive transmission lines. The exact new frequency positions of the transmission zeros and the central frequency of the passband can be calculated numerically by solving transcendental equations derived from (17) for specified C, ω_{EZ1}, ω_{EZ2} and z_c. The lowest and the highest achievable value of z_c depends on the substrate characteristics and transmission lines type. For microstrip lines it ranges typically from 0.4 to 3.

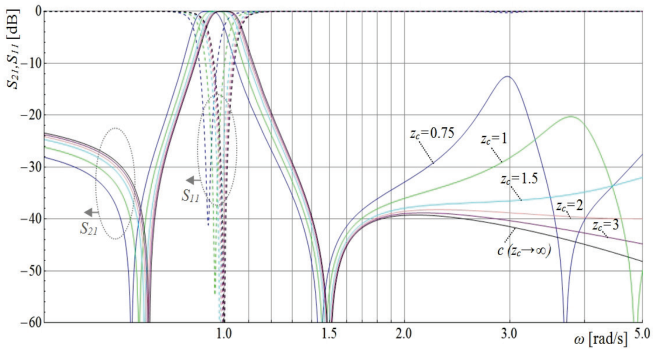

Fig. 5. Frequency characteristics of the filter with transmission lines of various z_c for $C = 4$, $\omega_{EZ1} = 0.75$ and $\omega_{EZ2} = 1.5$

IV. Filter With Transmission Lines as Dual Band Bandpass Filters

The feature of the filter with antiparallel configuration with transmission lines that is described in the previous section can be employed for the designing of filters with dual passbands by tuning the input parameters to obtain an additional passband with a small insertion loss and good matching.

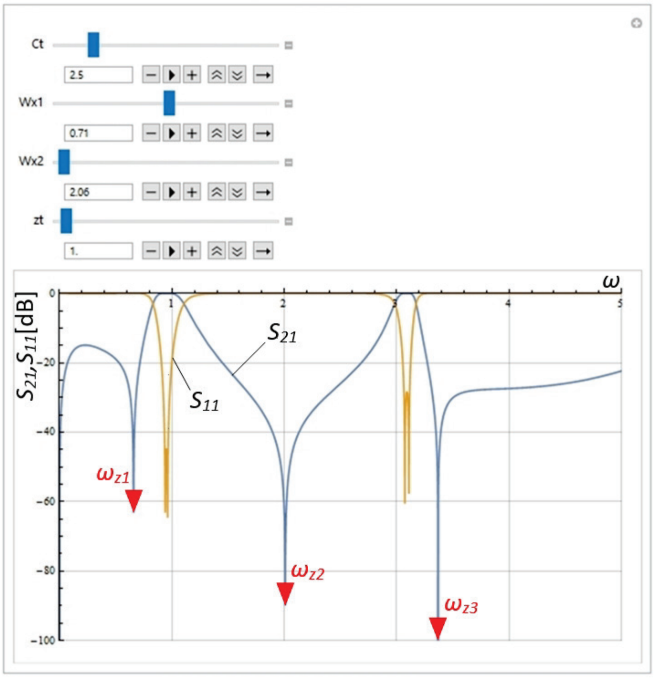

Fig. 6. Frequency characteristics of the filter with antiparallel configuration with corresponding values of independent variables Ct (C), Wx1 (ω_{EZ1}), Wx2 (ω_{EZ2}), and zt (z_c) example 1

Fig. 6 and Fig. 7 show two examples of dual band frequency characteristics obtained by [11] for two different sets of independent variables C, ω_{EZ1}, ω_{EZ2} and z_c.

These examples demonstrate that dual band filters with a different frequency distance between the first and second passband and with various bandwidths can be obtained. Since the major objective is to achieve low insertion loss and good matching in both passbands, the position of the transmission zeros cannot be independently adjusted as in the case of the extended antiparallel filters from Section II. As explained in Section III, the transmission zeros positions (marked as ω_{Z1} and ω_{Z2} in Figs. 6 and 7) deviate from the values set by parameters ω_{EZ1} and ω_{EZ2}. This deviation increases as the characteristic impedance of the inductive transmission lines decreases. Dual band filters also acquire additional transmission zeros above the upper passbands, marked as ω_{Z3} in Figs. 6 and 7. The value of ω_{Z3} can also be calculated numerically by solving transcendental equations derived from (17) for specified C, ω_{EZ1}, ω_{EZ2} and z_c.

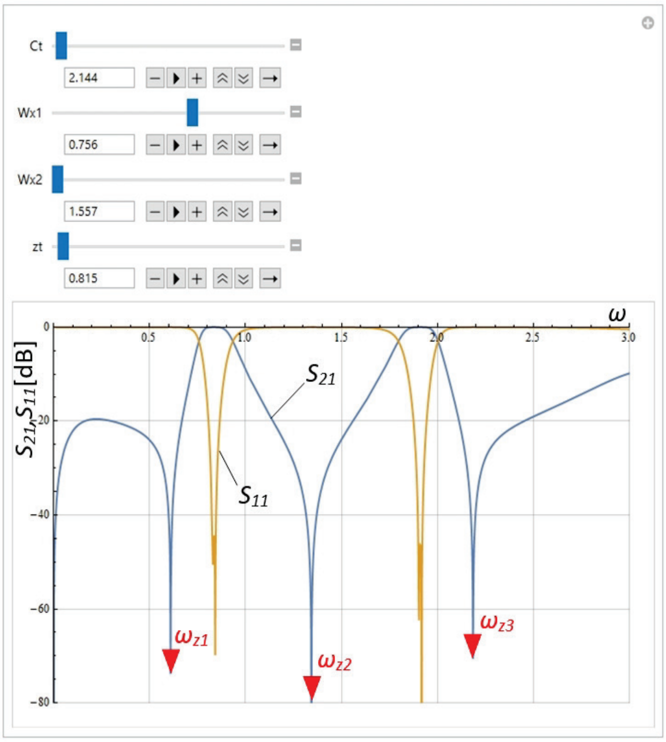

Fig. 7. Frequency characteristics of the filter with antiparallel configuration with corresponding values of independent variables Ct (C), Wx1 (ω_{EZ1}), Wx2 (ω_{EZ2}), and zt (z_c) example 2

The examples from Fig. 6 and Fig. 7 show that the lower values of parameter C are required for achieving dual band filter characteristics. Since the decreasing of parameter C also decreases the isolation in all stopbands, the single stage dual band filters with antiparallel configurations inevitably suffer from poor selectivity. Fortunately, as will be shown in the following sections, this category of filters could be easily cascaded for achieving multi-stage configuration with significantly increased selectivity.

V. Cascading of Antiparallel Networks

Due to their specific general topology, filters with antiparallel configurations can be cascaded in two different ways to obtain a two-stage filter as shown in Fig 8.

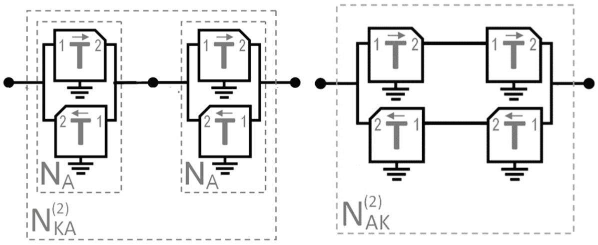

(a) (b)

Fig. 8. The cascade connection: (a) of two antiparallel networks (KA config.) and (b) of two pairs of cascaded subnetworks (AK configuration) [12]

If expressed in terms of the elements of the transmission matrix of the fundamental subnetworks, both transmission matrices of the two-stage networks from Fig.8 are identical:

$$\mathbf{T}_{\mathbf{KA}}^{(2)} = \mathbf{T}_{\mathbf{AK}}^{(2)} = \begin{bmatrix} \dfrac{(A+D)^2-2}{2} & \dfrac{B(A+D)}{2} \\ \dfrac{(A+D)\left((A+D)^2-4\right)}{2B} & \dfrac{(A+D)^2-2}{2} \end{bmatrix}. \tag{18}$$

This means that these two different topologies are electrically equivalent. However, general planar topologies of these two different configurations are significantly different as shown in Fig. 9 and Fig 10.

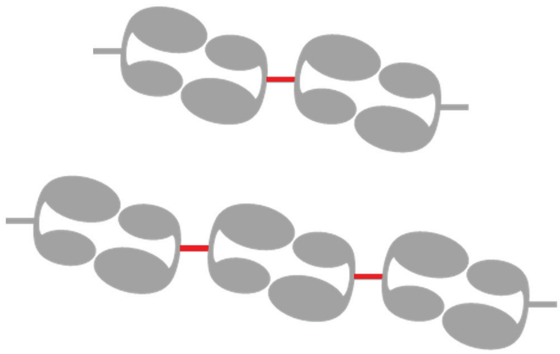

Fig. 9. General planar topology of two-stage (above) and three-stage (below) multistage filters with KA configuration [12]

The planar topology from Fig. 9 suffers from an inherent drawback regarding the connection between the adjacent stages, which are marked with red connecting lines. Since the equation (18) for the transmission matrix of the cascade does not include these lines, their electrical length should be zero, while for the separation of the adjacent resonator the length of these lines should be (significantly) larger than zero. Equation (18) can be expanded by including a transmission matrix that describes the influence of the non-zero transmission lines, however the frequency characteristics of the overall multistage filters will be degenerated, which will also be the case with the characteristics of a realized planar filter having the topology from Fig. 9. The topology from Fig. 10 does not require the connection lines between the adjacent stages and therefore is much more suitable for practical realization.

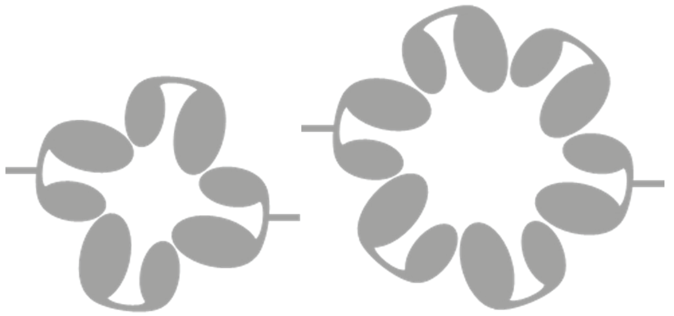

Fig. 10. General planar topology of two-stage (left) and three-stage (right) multistage filters with AK configuration [12]

By introducing the substitutions $p=(A+D)/2$ and $q=B/(2Z_0)$, the S-parameter matrix of the single-stage antiparallel network, expressed in terms of the ABCD elements of the fundamental subnetwork's transmission matrix, becomes:

$$\mathbf{S_A}=\begin{bmatrix} S_{11} & S_{12} \\ S_{21} & S_{22}\end{bmatrix}, \tag{19}$$

where:

$$S_{11}=S_{22}=\frac{BS_{11}^{(1)}}{IS^{(1)}}=\frac{q^2-p^2+1}{(q+p)^2-1} \text{ and } S_{12}=S_{21}=\frac{BS_{21}^{(1)}}{IS^{(1)}}=\frac{q}{(q+p)^2-1}$$

Using the same substitutions, the S-parameter matrix for the double-stage antiparallel filter can be calculated from (18) as:

$$\mathbf{S}_{\mathbf{A}}^{(2)}=\begin{bmatrix} S_{11}^{(2)} & S_{12}^{(2)} \\ S_{21}^{(2)} & S_{22}^{(2)}\end{bmatrix}, \tag{20}$$

where:

$$S_{11}^{(2)}=S_{22}^{(2)}=\frac{BS_{11}^{(2)}}{IS^{(2)}}=\frac{p\left(q^2-p^2+1\right)}{\left((q+p)^2-1\right)p-q}=\frac{p\cdot BS_{11}^{(1)}}{p\cdot IS^{(1)}-q},$$

$$S_{12}^{(2)}=S_{21}^{(2)}=\frac{BS_{21}^{(2)}}{IS^{(2)}}=\frac{q}{\left((q+p)^2-1\right)p-q}=\frac{BS_{21}^{(1)}}{p\cdot IS^{(1)}-q}.$$

By successively applying the same procedure a recurrent expression for S-parameter matrix for a multi stage antiparallel filter of arbitrary rank (r) can be obtained as:

$$\mathbf{S}_{\mathbf{A}}^{(r)}=\begin{bmatrix} S_{11}^{(r)} & S_{12}^{(r)} \\ S_{21}^{(r)} & S_{22}^{(r)}\end{bmatrix}, \tag{21}$$

where:

$$S_{11}^{(r)}=S_{22}^{(r)}=\frac{BS_{11}^{(r)}}{IS^{(r)}}=\frac{\left(q^2-p^2+1\right)\cdot \mathbf{U}_{r-1}(p/2)}{p\cdot IS^{(r-1)}-q},$$

$$S_{12}^{(r)}=S_{21}^{(r)}=\frac{BS_{21}^{(r)}}{IS^{(r)}}=\frac{q}{p\cdot IS^{(r-1)}-q}=\frac{BS_{21}^{(1)}}{p\cdot IS^{(r-1)}-q}.$$

The expression $U_{r-1}(p/2)$ in the nominator of S_{11} is a Chebyshev polynomial of the second kind having a general form given with the expression:

$$\mathbf{U}_{r-1}\left(\frac{p}{2}\right)=\frac{2\sin\left(r\cdot\arccos(p/2)\right)}{\sqrt{4-p^2}}. \tag{22}$$

Such a polynomial of the rank r-1 has r-1 different real zeros defined by the expression:

$$p_{r-1,l}=\cos\left(\frac{l\pi}{r}\right), \quad \text{for } l=1 \text{ to } r\text{-1}. \tag{23}$$

Comparing the equations (19), (20) and (21) shows that the nominator of S_{21} (and S_{12}) remains unchanged regardless of the filter's rank. Because of that, the number and the frequency positions of the transmission zeros will remain unchanged regardless of the rank of the filter.

However, the comparison of the nominators of S_{11} (and S_{12}) in the equations (19) and (20) shows that the number of S_{11} zeros, which are in the same time poles of S_{21}, could increase. Besides the poles that exist in the case of the single-stage antiparallel filter, defined by the solution of the equation:

$$\left|q^2-p^2+1\right|=0. \tag{24}$$

Two stage filters will have an additional pole defined by the solution of the equation:

$$p=\frac{A+D}{2}=0. \tag{24}$$

Equations (7-9) show that the number of poles in a multi-stage antiparallel filter increases by one for every additional stage. The frequency position of the additional cascade poles can be calculated by solving the following equation:

$$\frac{A+D}{2}-\cos\left(\frac{l\pi}{r}\right)=0 \qquad \text{for } l=1 \text{ to } r\text{-1}. \tag{25}$$

By applying (25) for EABPF, the equation for all cascade poles can be obtained as:

$$\omega_{kp(r-1,l)}=\sqrt{\frac{2+k(1+mCL+n)-2\cos(l\pi/r)}{k((m+1)CL+n)}}, \text{ for } l=1 \text{ to } r\text{-1}. \tag{26}$$

Fig. 11 shows the frequencies of all multi-stage EABPF poles for filter ranks from 1 to 10 and one set of filter parameters.

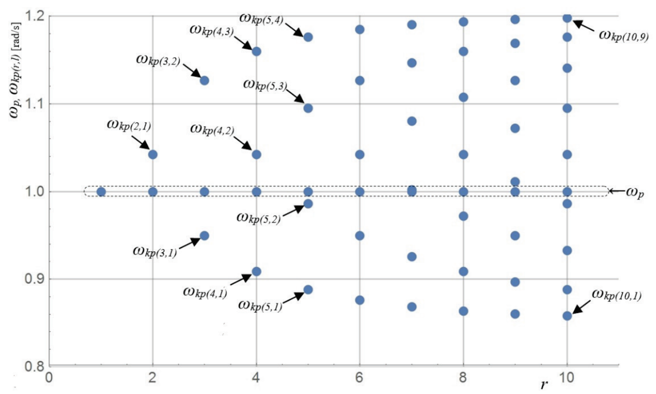

Fig. 11. Pole frequencies of multi-stage EABPFs for cascade rank from 1 to 10 for the independent parameter value C = 4, and frequency zeros positions ω_{EZ1} = 0.5 and ω_{EZ2} = 2 [12]

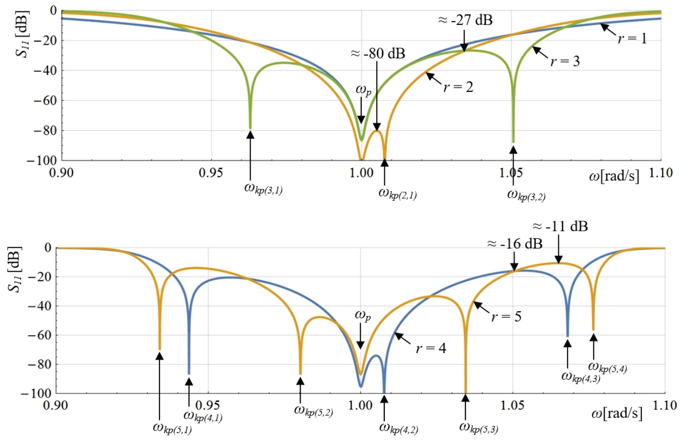

Fig. 12. Frequency characteristics of S_{11} of EABPF for cascade ranks: r = 1 to 3 (top) and r = 4 to 5 (bottom), for the independent parameter value C = 4, and frequency zeros positions ω_{EZ1} = 0.5 and ω_{EZ2} = 2 [12]

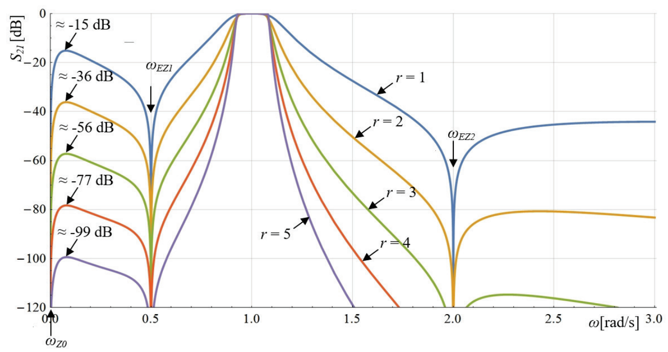

Fig. 13. Frequency characteristics of S_{21} of EABPF for cascade ranks: r = 1 to 5 and for the independent parameter value C = 4, and frequency zeros positions ω_{EZ1} = 0.5 and ω_{EZ2} = 2 [12]

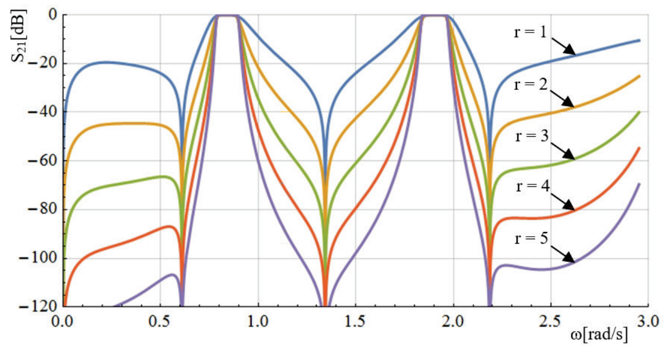

Fig. 14. Frequency characteristics of S_{21} of EABPF for cascade ranks: r = 1 to 5 and for the values of independent variables the same as in example 2, shown in Fig. 7

Figs. 12 and 13 show S parameters frequency characteristics for several multi stage EAPBF of various ranks. Fig. 12 shows positions of the transmission poles that perfectly correspond to values obtained by (18) and are shown in Fig. 11.

Fig. 13 shows S_{21} frequency characteristics of multi-stage EAPBF having the rank from r=1 to r=5. As predicted based on (19-21), the position of the transmission zeros (ω_{EZ1} and ω_{EZ2}) remains unchanged regardless of the filter order increase. Also, the filter selectivity increases rapidly with the increase of the filter's rank. In that manner, the isolation minimum within the lower stopband, between the transmission zeros ω_{Z0} and ω_{EZ1}, increases rapidly from ≈15 dB for r = 1, to close to 100 dB for r = 5.

Fig. 14 displays S_{21} characteristics of dual band multi-stage EAPBF having the rank from r=1 to r=5 and independent filter's variables identical as for the example from Fig. 7. It shows that the selectivity of dual band filters with antiparallel configuration could be increased rapidly by the cascading of identical basic filters.

VI. Conclusion

Simple passive networks with antiparallel configurations could be employed for obtaining dual band filters with various frequency distances between the first and second passband. Also, basic band pass filters with antiparallel configurations could be cascaded for obtaining filters with higher selectivity. It was shown that this class of filters can be cascaded in two electrically equivalent ways, diverse in topology. The number and position of the transmission zeros remain unchanged with the increase of a filter's rank, while the number of transmission poles increases by one with every additional filter's stage. This feature can be employed for obtaining both single and dual bandpass filters with high selectivity.

Acknowledgement

This paper was supported by the Ministry of Education, Science and Technological Development of the Republic of Serbia under grant TR-32052.

This is an extended version of the paper "Concept of Dual-Band Bandpass Filters with Antiparallel Configuration" presented at 4th International Conference on Electrical, Electronic and Computing Engineering - IcETRAN 2017, held in Kladovo, Serbia. The paper has been awarded as the best paper presented in the Section Microwave Technique, Technologies and Systems.

References

[1] H. Miyake, S. Kitazawa, T. Ishizaki, T. Yamada, and Y. Nagatom, "A Miniaturized Monolithic Dual Band filter Using Ceramic Lamination Technique for Dual Mode Portable Telephones", *IEEE MTT-S Int. Dig.*, vol. 2, pp. 789–792, June 1997.

[2] A. Abbosh, "Design Method for Ultra-Wideband Bandpass Filter with Wide Stopband using Parallel-Coupled Microstrip Lines", *IEEE Transactions on Microwave Theory and Techniques*, vol. 60, no. 1, pp. 31–38, January 2012.

[3] S. Sun, "A Dual-Band Bandpass Filter using a Single Dual-Mode Ring Resonator", *IEEE Microwave Wireless Component Letters*, vol. 21, no. 6, pp. 298–300, June 2011.

[4] X.Y. Zhang and Q. Xue, "Harmonic-Suppressed Bandpass Filter Based on Discriminating Coupling", *IEEE Microwave Wireless Component Letters*, vol. 19, no. 11, pp. 695–697, November 2009.

[5] S. Sun and L. Zhu, "Compact Dual-Band Microstrip Bandpass Filter without External Feeds", *IEEE Microwave Wireless Component Letters*, vol. 15, no. 10, pp. 644–646, October 2005.

[6] S.B. Zhang and L. Zhu, “Synthesis Design of Dual-Band Bandpass Filters with λ/4 Stepped-Impedance Resonators”, *IEEE Transactions on Microwave Theory and Techniques*, vol. 61, no. 5, pp. 1812–1819, May 2013.
[7] S. Jovanović, B. Milovanović, and M. Gmitrović, "Theory and Realization of Simple Bandpass Filters with Antiparallel Configuration", *Progress in Electromagnetics Research*, vol. 136, pp. 101-122, 2013.
[8] S. Jovanović and V. Pantović, „Approximate Modelling Methods for Single-Stage Band Pass Filters with Antiparallel Configuration“, *12th International Conference on Telecommunications in Modern Satellite, Cable and Broadcasting Services - TELSIKS 2015*, Niš, Serbia, October 14-17, 2015, pp. 193-196.
[9] S. Jovanović, “Extended Configuration of Antiparallel Band Pass Filters with Two Independently Adjustable Transmission Zeros“, *Microwave Review*, vol. 19, no.1, September 2013, pp. 14-19.
[10] S. Jovanović and B. Milovanović, “General Planar Topologies of Single-Stage Band Pass Filters with Antiparallel Configuration“, *2nd International Conference on Electrical, Electronic and Computing Engineering - IcETRAN 2015*, Silver Lake, Serbia, June 8–11, 2015.
[11] http://www.wolfram.com/mathematica/
[12] S. Jovanović, V. Pantović and B. Milovanović, “General Properties of Multistage Bandpass Filters with Antiparallel Configuration“, *2017 13th International Conference on Advanced Technologies, Systems and Services in Telecommunications (TELSIKS)*, Niš, Serbia, 2017, pp. 158-161.